Two Closely Related Intersecting Tunnel Structures: The Monophosphates $K_3V_{1.4}W_{2.6}O_9(PO_4)_2$ and $K_3Nb_3WO_9(PO_4)_2$

F. Berrah,[†] D. Mezaoui,[‡] A. Guesdon,[†] M. M. Borel,[†] A. Leclaire,*[,†] J. Provost,[†] and B. Raveau[†]

Laboratoire CRISMAT, UMR 6508 associée au CNRS, ISMRA et Université de Caen, 6, Boulevard du Maréchal Juin, 14050 CAEN Cedex, France, and Laboratoire de Cristallographie et Cristallogénèse, Institut de Chimie U.S.T.H.B, B.P. 32, El-Alia Bab-Ezzouar, Alger, Algeria

Received August 4, 1997. Revised Manuscript Received October 23, 1997

Two new monophosphates with original and closely related intersecting tunnel structures have been synthesized. The first one $K_3V_{1.4}W_{2.6}O_9(PO_4)_2$ crystallizes in the $P2_1/m$ space group with $a = 7.0392(6)$ Å, $b = 14.332(1)$ Å, $c = 7.5508(7)$ Å, $\beta = 106.320(8)°$, and the second one, $K_3Nb_3WO_9(PO_4)_2$, crystallizes in the $Pnma$ space group with $a = 14.667(2)$ Å, $b = 14.508(3)$ Å, $c = 7.179(1)$ Å. Their 3D-frameworks $[M_4P_2O_{17}]_\infty$ are built from the assemblage of octahedral $[MO_3]_\infty$ chains interconnected through "MPO_9" units. The two structures differ by the relative orientation of their $[MO_3]_\infty$ chains: in the "V, W" phase two successive chains are deduced from each other by a "$\vec{c}$" translation, whereas in the "Nb, W" phase one chain out of two is turned by 180° around $\vec{a}$. The analysis of these structures shows also their close relationships with the hexagonal tungsten bronze (HTB): the framework can also be described on the basis of HTB ribbons running along b. Another important feature deals with the tendency of the transition elements to order, especially in the $[MO_3]_\infty$, chains. The magnetic study of the mixed valent monophosphate $K_3V_2W_2O_9(PO_4)_2$ evidences electronic localization despite the existence of $[MO_3]_\infty$ chains.

Introduction

The investigations performed the past 20 years on reduced transition elements phosphates have evidenced the great richness of these compounds. If most of them present bi- or tridimensional frameworks, they exhibit very different structures depending on the nature of the transition element as exemplified by transition metal phosphates containing potassium.

Tungsten and niobium for instance often give rise to three-dimensional frameworks derived from the ReO_3-type or hexagonal tungsten bronze structures (see for a review refs 1 and 2), whereas molybdenum in most cases leads to isolated MoO_6 octahedra or to octahedral units built up from the association of a small number of octahedra (see for instance ref 3). In contrast, vanadium phosphates offer a great diversity in the connection of their VO_6 octahedra and VO_5 pyramids forming isolated polyhedra, polyhedral units, or octahedral rows of corner or edge-sharing octahedra (see for instance refs 4−8). This structural diversity of the phosphates of transition elements leads to various physical properties as electronic conductivity for the tungsten bronze phosphates, ionic conductivity in the case of the Nasicon-type compounds, or optical properties for the $KTiPO_5$ type structures.

Recent investigations of transition metal phosphates containing two transition elements in the same framework, i.e., molybdenum and tungsten, have allowed original structures, different from the "pure" molybdenum or tungsten phosphates, to be generated.[9−16] To prepare new materials, we have associated to tungsten a second element, vanadium or niobium, which can adopt like molybdenum several oxidation states and is susceptible to form, like Mo(V), vanadyl or niobyl bonds.

In the present paper we report on two potassium monophosphates, $K_3V_{1.4}W_{2.6}O_9(PO_4)_2$ and $K_3Nb_3WO_9$-

[†] Laboratoire CRISMAT.
[‡] Laboratoire de Cristallographie et Cristallogénèse.

(1) Raveau, B. *Proc. Ind. Acad. Sci.* **1989**, *96*, 419.
(2) Borel, M. M.; Goreaud, M.; Grandin, A.; Labbé, P.; Leclaire, A.; Raveau, B. *Eur. J. Solid State Inorg. Chem.* **1991**, *28*, 93.
(3) Canadell, E.; Provost, J.; Guesdon, A.; Borel, M. M.; Leclaire, A.; *Chem. Mater.* **1997**, *9*, 68.
(4) Kathuis, V. C.; Hoffmann, R. D.; Huang, J.; Sleight, A. W. *Chem. Mater.* **1993**, *5*, 206
(5) Lii, K. H.; Liu, W. C. *J. Solid State Chem.* **1993**, *103*, 38
(6) Wang, K.; Lii, K. H. *Acta Cryst* **1992**, *C48*, 975.
(7) Lii, K. H.; Mao, L. F. *J. Solid State Chem.* **1992**, *96*, 436.
(8) Phillips, M. L.; Harrison, W. T.; Gier, W. T.; Stucky, G. D.; Kulkarni, G. V.; Burdett, J. K. *Inorg. Chem.* **1990**, *29*, 2158.
(9) Leclaire, A.; Borel, M. M.; Chardon, J.; Raveau B. *Mater. Res. Bull.* **1995**, *30*, 1075.
(10) Leclaire, A.; Borel, M. M.; Chardon, J.; Raveau, B. *J. Solid State Chem.* **1995**, *120*, 353.
(11) Leclaire, A.; Borel, M. M.; Chardon, J.; Raveau B. *J. Solid State Chem.* **1996**, *124*, 224.
(12) Leclaire, A.; Borel, M. M.; Chardon, J.; Raveau, B. *J. Solid State Chem.* **1996**, *127*, 1.
(13) Leclaire, A.; Borel, M. M.; Chardon, J.; Raveau, B. *J. Solid State Chem.* **1997**, *128*, 191.
(14) Leclaire, A.; Borel, M. M.; Chardon, J.; Raveau, B. *J. Solid State Chem.* **1997**, *128*, 215.
(15) Leclaire, A.; Borel, M. M.; Chardon, J.; Raveau, B. *Mater. Res. Bull.* **1996**, *31*, 1257.
(16) Leclaire, A.; Borel, M. M.; Chardon, J.; Raveau, B. *J. Solid State Chem.* **1997**, *130*, 48.

S0897-4756(97)00547-4 CCC: $15.00
Published on Web 01/21/1998

Table 1. Cell Parameters for the Compounds $A_3V_2W_2O_9(PO_4)_2$ (A = K, Rb, Tl, Cs) and $A_3Nb_3WO_9(PO_4)_2$ (A = K, Rb, Cs)

compound	*a* (Å)	*b* (Å)	*c* (Å)	*β* (deg)	*V* (Å^3)
$K_3V_2W_2O_9(PO_4)_2$	7.070(1)	14.239(2)	7.57(1)	106.43(1)	728.8
$Rb_3V_2W_2O_9(PO_4)_2$	7.054(1)	14.243(4)	7.639(1)	105.73(2)	738.7
$Tl_3V_2W_2O_9(PO_4)_2$	7.049(1)	14.219(8)	7.601(4)	105.6(3)	733.8
$Cs_3V_2W_2O_9(PO_4)_2$	7.082(1)	14.317(4)	7.773(3)	105.52(2)	759.4
compound	*a* (Å)	*b* (Å)	*c* (Å)		*V* (Å^3)
$K_3Nb_3WO_9(PO_4)_2$	14.667(2)	14.508(3)	7.179(1)		1527.6
$Rb_3Nb_3WO_9(PO_4)_2$	14.905(1)	14.534(1)	7.192(1)		1558.0
$Cs_3Nb_3WO_9(PO_4)_2$	15.152(1)	14.596(1)	7.255(5)		1604.5

Table 2. Summary of Crystal Data, Intensity Measurements, and Structure Refinement Parameters

	$K_3V_{1.4}W_{2.6}O_9(PO_4)_2$	$K_3Nb_3WO_9(PO_4)_2$
space group	$P2_1/m$ (No. 11)	*Pnma* (No. 62)
cell dimensions	$a = 7.0392(6)$ Å	$a = 14.667(2)$ Å
	$b = 14.332(1)$ Å	$b = 14.508(3)$ Å
	$c = 7.5508(7)$ Å	$c = 7.179(1)$ Å
	$\beta = 106.320(8)°$	
volume (Å)^3	734.2(1)	1527.6(4)
Z	2	4
ρ_{calc} (g.cm^{-3})	4.53	4.00
λ (Mo Kα)	0.710 73	0.710 73
scan mode	$\omega-\theta$	$\omega-\theta$
scan width (deg)	$1.0 + 0.35 \tan\theta$	$1.6 + 0.35 \tan\theta$
slit aperture (mm)	$1.0 + \tan\theta$	$1.4 + \tan\theta$
max θ (deg)	45	45
standard reflections	3 measured every 3600 s	3 measured every 3600 s
measured reflections	6478	6925
reflections with $I > 3\sigma$	668	656
μ (mm^{-1})	22.3	10.9
parameters refined	72	81
agreement factors	$R = 0.046$	$R = 0.054$
	$R_w = 0.038$	$R_w = 0.048$
weighting scheme	$w = 1/(\sigma(F))^2$	$w = 1/(\sigma(F))^2$

$(PO_4)_2$, with original and closely related intersecting tunnel structures.

Crystal Growth and Chemical Synthesis

The Monophosphate $K_3V_{1.4}W_{2.6}O_9(PO_4)_2$. Single crystals of this phase were grown from a mixture of nominal composition $K_5V_{1.7}W_{1.7}P_{1.6}O_{15}$. The growth was performed in two steps: first, $H(NH_4)_2PO_4$, K_2CO_3, V_2O_5, and WO_3 were mixed in adequate ratios according to the composition $K_5V_{1.7}W_{1.416}P_{1.6}O_{15}$ and heated in a platinum crucible for 4 h at 673 K in air in order to decompose the ammonium phosphate and the potassium carbonate. The required amount of tungsten (0.284 mol) was then added, and the resulting mixture was sealed in an evacuated silica ampule. It was heated at 883 K for 18 h, cooled at 3.33 K/h down to 683 K, and finally quenched to room temperature.

Attempts to prepare isotypic compounds with different V/W ratios in the form of monophasic powder were successful only for the composition $K_3V_2W_2O_9(PO_4)_2$. $A_3V_2W_2(PO_4)_2$ phosphates have also been prepared for A = Rb, Tl, and Cs. All these compounds were prepared as we described above, heated at 853 K for 10 h, cooled at 20 K/h down to 653 K, and then quenched to room temperature. Note that either vanadium or tungsten can be used as reducer. The X-ray powder diffraction of the different $A_3V_2W_2O_9(PO_4)_2$ phases (A = K, Rb, Tl, and Cs) have been indexed in the $P2_1/m$ space group, allowing the calculation of the cell parameters given in Table 1.

The Monophosphate $K_3Nb_3WO_9(PO_4)_2$. Single crystals of $K_3Nb_3WO_9(PO_4)_2$ were grown from a mixture of nominal composition $K_4Nb_2W_2P_2O_{17}$. The synthesis was performed in a similar way as for the previous phases except that Nb_2O_5 was used instead of V_2O_5. The mixture was heated for 12 h at 1073 K, cooled at 12.5 K/h down to 773 K, and finally quenched to room temperature.

From the resulting mixture some blue plates were extracted. The microprobe analysis of several crystals confirmed the composition $K_3Nb_3WP_2O_{17}$ deduced from the structure determination.

Attempts to prepare $A_3Nb_3WO_9(PO_4)_2$ in the form of a pure powder were successful for A = K, Rb, and Cs. The synthesis of the latter was performed in air from the nominal composition by heating at 1153 K for 12 h and quenching to room temperature. The results were the expected powders, the X-ray patterns were indexed and led to the cell parameters of Table 1.

Note that attempts to synthesize compounds with a ratio Nb/W < 3 always led to polyphasic samples.

Determination of the Structure

The selection of the crystals was carried out by testing the different crystals that were optically good, by the Weissenberg method. The cell parameters (Table 2) were determined by diffractometric techniques at 294 K with a least-squares refinement based upon 25 reflections in the range $18° < \theta < 22°$.

For the data collections with a CAD4 Enraf Nonius diffractometer, a mauve platelet with dimensions 0.0257 × 0.0257 × 0.0129 mm for the vanadium compound and a blue platelet with dimensions 0.0720 × 0.0308 × 0.0142 mm for the niobium compound were used. The parameters of the data collections are reported on Table 2. The reflections were corrected for Lorentz and polarization effects and for absorption. Both structures were solved with the heavy atom method.

For the vanadium compound, the systematic absences $k = 2n + 1$ for $0k0$ are compatible with the space groups $P2_1$ and $P2_1/m$.

The Harker peaks in the Patterson function are characteristic of the centrosymmetric group $P2_1$/m. The refinements of the atomic coordinates and of the thermal factors of all the atoms and of the occupancy factors of the atoms located in the octahedra and tetrahedra led to the formulation $K_3V_{1.41}W_{2.59}P_2O_{17}$ and to the positional parameters listed in Table 3a with $R = 0.046$ and $R_w = 0.038$. For the oxygen atom O(8) the refined thermal factors have no physical signification so we fixed $U_{iso} = 0.005$ without any refinement of this value.

For the niobium compound the systematic absences $k + l = 2n + 1$ for $0kl$ and $h = 2n + 1$ for $hk0$ are consistent with the space groups *Pnma* and $Pn2_1a$. The Harker peaks in the Patterson function are characteristic of the centrosymmetric group *Pnma*. The refinements were conducted as in the vanadium compound. They led to the formulation $K_3Nb_3WP_2O_{17}$ and to the atomic parameters listed in Table 3b with $R = 0.054$ and $R_w = 0.048$.

The $[V_{1.4}W_{2.6}P_2O_{17}]_\infty$ and $[Nb_3WP_2P_{17}]_\infty$ Host Lattices

The projections of these structures along $\vec{b}$ for $K_3V_{1.4}W_{2.6}O_9(PO_4)_2$ (Figure 1a) and for $K_3Nb_3WO_9(PO_4)_2$

Table 3. Positional Parameters and Their Estimated Standard Deviations[a]

(a) $K_3V_{1.4}W_{2.6}O_9(PO_4)_2$[b]

atom	*x*	*y*	*z*	U_{eq} (Å^2)	site
W(1)	0.9787(3)	3/4	0.4790(3)	0.0079(8) *	2e
M(2)	0.4876(4)	3/4	0.4534(4)	0.009(1) *	2e
M(3)	0.2013(3)	0.1242(1)	0.1780(2)	0.0099(7) *	4f
P(1)	0.149(1)	0.6034(5)	0.203(1)	0.006(1)	4f
K(1)	0.602(2)	1/4	0.051(2)	0.039(3)	2e
K(2)	0.706(1)	0.5179(6)	0.311(1)	0.048(3)	4f
O(1)	0.969(3)	0.657(1)	0.637(2)	0.010(4)	4f
O(2)	0.254(4)	3/4	0.526(4)	0.006(5)	2e
O(3)	0.705(4)	3/4	0.356(4)	0.018(7)	2e
O(4)	0.997(3)	0.654()	0.278(2)	0.014(4)	4f
O(5)	0.346(3)	0.845(1)	0.248(2)	0.015(4)	4f
O(6)	0.409(3)	0.150(1)	0.390(2)	0.015(4)	4f
O(7)	0.338(2)	0.086(1)	0.042(2)	0.016(5)	2e
O(8)	0.188(3)	1/4	0.112(3)	0.005	4f
O(9)	−0.075(2)	0.100(1)	0.006(2)	0.010(4)	4f
O(10)	0.179(3)	−0.002(2)	0.291(3)	0.020(5)	4f

(b) $K_3Nb_3WO_9(PO_4)_2$

atom	*x*	*y*	*z*	U_{eq} (Å^2)	site
M(1)	0.2774(2)	1/4	0.3289(6)	0.009(1)*	4c
M(2)	0.2408(2)	3/4	0.3418(4)	0.0035(8)*	4c
M(3)	0.0886(2)	0.3774(1)	0.1332(3)	0.0058(7)*	8d
P(1)	0.1013(5)	0.6038(5)	0.097(1)	0.008(2)	8d
K(1)	0.4827(9)	3/4	0.065(3)	0.045(5)*	4c
K(2)	0.3463(6)	0.4864(8)	0.114(3)	0.057(4)*	8d
O(1)	0.132(1)	0.654(1)	−0.084(3)	0.008(4)	8d
O(2)	0.194(1)	0.345(1)	0.279(4)	0.019(6)	8d
O(3)	0.263(2)	3/4	0.089(3)	0.005(5)	4c
O(4)	0.326(2)	1/4	0.083(4)	0.008(6)	4c
O(5)	0.189(1)	0.346(1)	−0.097(3)	0.007(5)	8d
O(6)	0.134(1)	0.655(1)	0.275(5)	0.019(6)	8d
O(7)	0.003(1)	0.404(1)	−0.089(3)	0.006(4)	8d
O(8)	0.138(1)	0.506(1)	0.092(3)	0.007(5)	8d
O(9)	0.057(2)	1/4	0.139(5)	0.017(8)	4c
O(10)	0.023(1)	0.413(1)	0.321(3)	0.017(5)	8d

[a] Starred atoms have been refined anisotropically. Anisotropically refined atoms are given in the form of the isotropic equivalent displacement parameter defined as $U_{eq} = \sum_i \sum_j U^{ij} a_i^* a_j^* \mathbf{a}_i \mathbf{a}_j$. [b] M(2) = 0.41(1)V + 0.59(1)W. M(3) = 0.501(8)V + 0.499(8)W. [c] M(1) = 0.89(2)Nb + 0.11(2)W. M(2) = 0.46(2)Nb + 0.54(2)W. M(3) = 0.84(2)Nb + 0.16(2)W.

(Figure 1b), show that the two frameworks $[M_4P_2O_{17}]_\infty$ (M = V, Nb, W) exhibit a great similarity although the compounds crystallize in different space groups. Both structures are built up of $[MO_3]_\infty$ chains of corner-sharing octahedra running along $\vec{a}$ for the "V, W" phase, and along $\vec{c}$ for the "Nb, W" compound. These chains exhibit a similar arrangement in the two structures, i.e., they are spaced by about 7−7.3 Å in the (010) plane (Figure 1) and by about 7.2 Å along $\vec{b}$ (see projections of the structures along $\vec{b}$ (Figure 2a) and along $\vec{c}$ (Figure 2b). In both frameworks the $[MO_3]_8$ chains are interconnected through similar units "PMO_9" of two polyhedra, i.e., one MO_6 octahedron and one PO_4 tetrahedron sharing one apex (see inserts in Figures 1 and 2).

In fact both structures can be described by the stacking along $\vec{b}$ of $[M_4P_2O_{19}]_\infty$ layers built up of the $[MO_3]_\infty$ chains interconnected through "MPO_9" units (Figure 3). However the two structures differ by the relative orientations of the $[MO_3]_\infty$ chains. In the "V, W" monophosphate two successive $[MO_3]_\infty$ chains in a (010) layer (Figure 3a) are deduced one from the other by a single translation along $\vec{c}$, whereas in the "Nb, W" compound one chain out of two is turned by 180° around $\vec{a}$ (Figure 3b). Consequently, the nine-sided C-shaped windows generated by this assemblage are all oriented

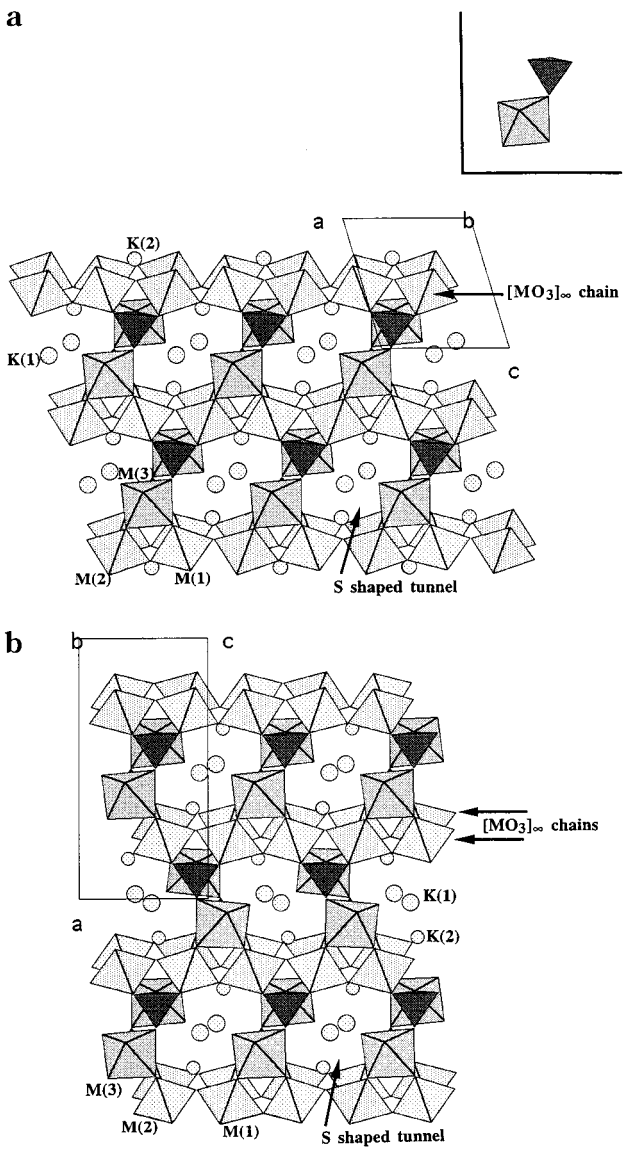

Figure 1. (a) Projection of the structure of $K_3V_{1.4}W_{2.6}O_9(PO_4)_2$ along $\vec{b}$. (b) Projection of the structure of $K_3Nb_3WO_9(PO_4)_2$ along $\vec{b}$.

in the same direction in $K_3V_{1.4}W_{2.6}O_9(PO_4)_2$ (Figure 3a) whereas they form a fish-bone array in $K_3Nb_3WO_9(PO_4)_2$ (Figure 3b).

In both structures, the $[M_4P_2O_{19}]_\infty$ layers parallel to (010) are stacked along $\vec{b}$ in the following way: one layer out of two is turned by 180° around $\vec{b}$ so that the PO_4 tetrahedra of each layer can share one apex with the MO_6 octahedra of the adjacent layers (Figure 2a,b). The comparison of the projections of $K_3V_{1.4}W_{2.6}O_9(PO_4)_2$ along $\vec{a}$ (Figure 2a) and of $K_3Nb_3WO_9(PO_4)_2$ along $\vec{c}$ (Figure 2b) evidences the great similarity between the two structures. The two resulting $[M_4P_2O_{17}]_\infty$ host lattices exhibit intersecting tunnels in which the potassium cations are located:

(i) Pentagonal and distorted hexagonal tunnels, running along $\vec{a}$ in the vanadium compound (Figure 2a) and along $\vec{c}$ in the niobium one (Figure 2b).

(ii) Along $\vec{b}$, S-shaped tunnels are observed, all being in the same orientation in $K_3V_{1.4}W_{2.6}O_9(PO_4)_2$ (Figure 1a), whereas they present a fish-bone array in $K_3Nb_3WO_9(PO_4)_2$ (Figure 1b).

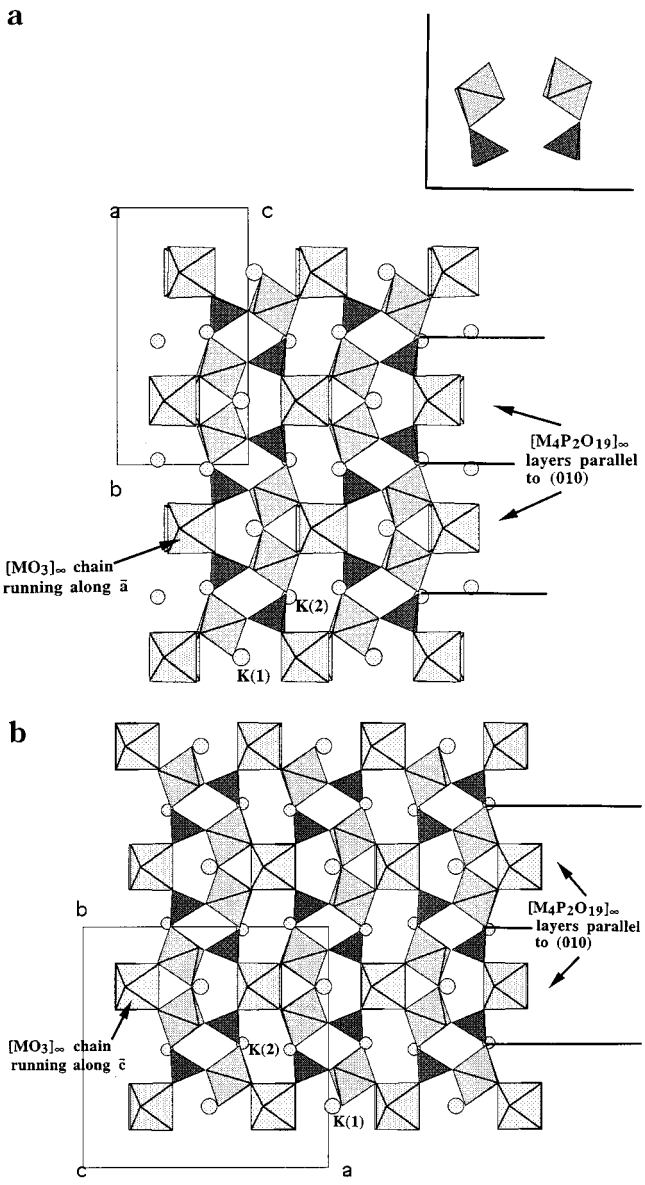

Figure 2. (a) Projection of the structure of $K_3V_{1.4}W_{2.6}O_9(PO_4)_2$ along $\vec{a}$. (b) Projection of the structure of $K_3Nb_3WO_9(PO_4)_2$ along $\vec{c}$.

(iii) Large tunnels resulting from the stacking of brownmillerite windows exist along the [101] direction in $K_3V_{1.4}W_{2.6}O_9(PO_4)_2$ (Figure 4a); in $K_3Nb_3WO_9(PO_4)_2$ they are partially obstructed because of the shift of one $[M_4P_2O_{21}]_\infty$ chain out of two, which gives rise to zigzag tunnels in this direction (Figure 4b).

(iv) Finally, in a similar way, six-sided tunnels are observed along $\vec{c}$ in the vanadium compound (Figure 5), whereas no tunnel is observed along $\vec{a}$ for the niobium monophosphate.

Relationships with the Hexagonal Tungsten Bronze (HTB) Structure

The O−O−O angles close to 120−60° between the MO_6 octahedra formed by the $[MO_3]_\infty$ chains (Figure 1) remind us the geometry of the HTB structure, already observed for niobium phosphate bronzes[17] and also for $KVPO_5$.[18] In fact the entire host lattice of these compounds can be described by the assemblage of HTB type ribbons running along $\vec{b}$. Each ribbon (Figure 6b)

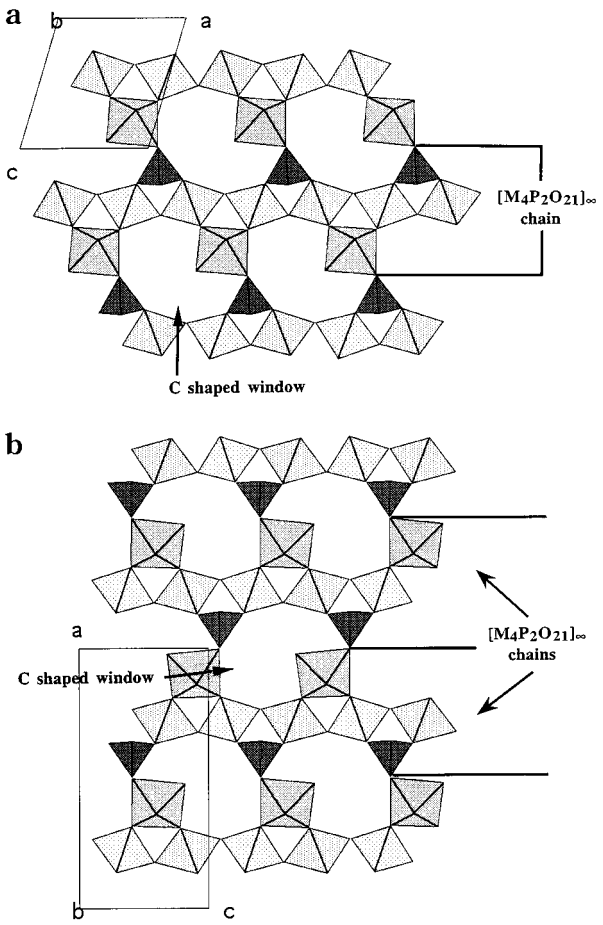

Figure 3. (a) One $[M_4P_2O_{19}]_8$ layer parallel to (010) in $K_3V_{1.4}W_{2.6}O_9(PO_4)_2$. (b) One $[M_4P_2O_{19}]_8$ layer parallel to (010) in $K_3Nb_3WO_9(PO_4)_2$.

can be deduced from the pure octahedral HTB ribbon (Figure 6a) by replacing two octahedra out of six in an ordered way by two PO_4 tetrahedra. In both structures, the HTB type ribbons are oriented parallely to the (101) and (10$\bar{1}$) planes. They form stairs like infinite layers parallel to (001) in the "V, W" monophosphate (Figure 7a), and parallel to (100) in the "Nb, W" monophosphate (Figure 7b). The two structures differ only by the relative positions of the successive layers with respect to each other.

Distribution and Coordination of the Transition Elements

Three sites are available for the transition elements in the two structures. The first important point concerns the ordered character of the distribution of these elements in the $[MO_3]_\infty$ chains (Table 3). In the "V, W" monophosphate, one site of two, M(1), is fully occupied by tungsten, whereas the second site M(2) is almost occupied at random (41% V and 59% W; Table 3a). In the "Nb, W" monophosphate, the M(1) site is preferentially occupied by niobium (89% Nb + 11% W), whereas the second site is almost statistically occupied (46% Nb

(17) Raveau, B.; Borel, M. M.; Leclaire, A.; Grandin, A. *Int. J. Mod. Phys.* **1993**, *B7*, 4109

(18) Benhamada, L.; Grandin, A.; Borel, M. M.; Leclaire, A.; Raveau, B. *Acta Crystallogr.* **1991**, *C47*, 1137.

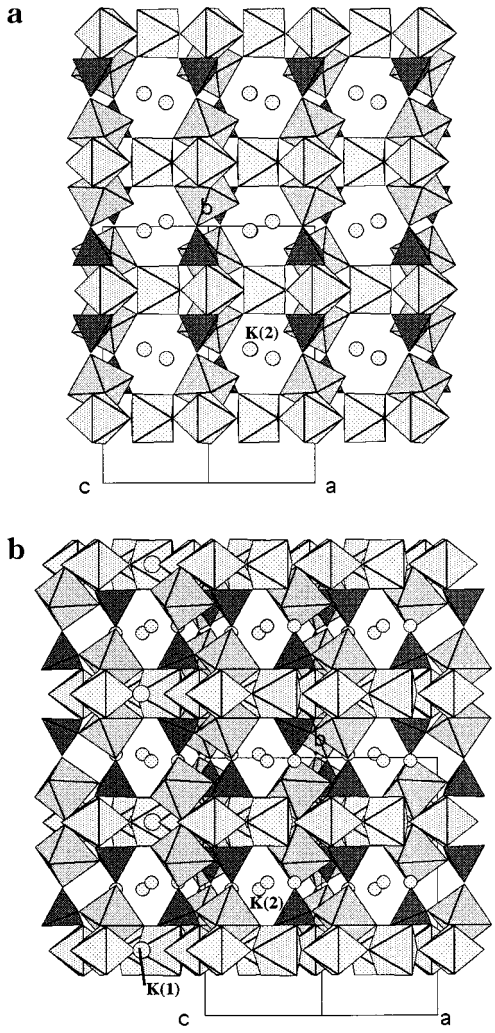

Figure 4. (a) Projection of the structure of $K_3V_{1.4}W_{2.6}O_9(PO_4)_2$ along [101]. (b) Projection of the structure of $K_3Nb_3WO_9(PO_4)_2$ along [101].

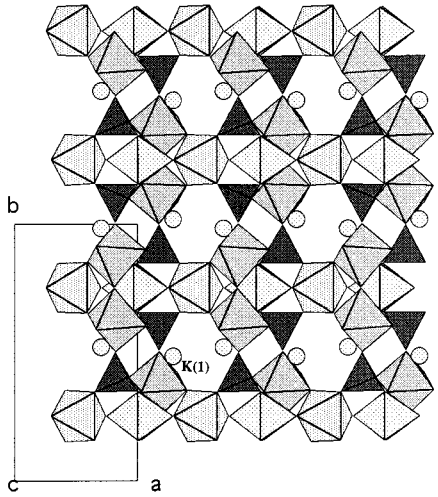

Figure 5. Projection of the structure of $K_3V_{1.4}W_{2.6}O_9(PO_4)_2$ along $\vec{c}$.

+ 54% W; Table 3b). The M(3) octahedra that form the "MPO_9" units located outside of the $[MO_3]_\infty$ chains exhibit occupancy rates of 50% V and 50% W for the "V, W" phase, against 84% Nb and 16% W for the "Nb, W" compound.

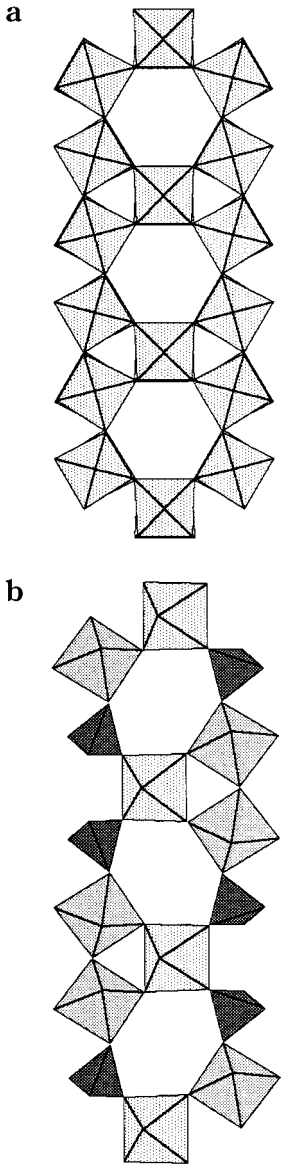

Figure 6. Ideal configuration of the hexagonal tungsten bronze HTB type ribbons (a) in the pure octahedral bronzes and (b) in the "KVW" and "KNbW" monophosphate.

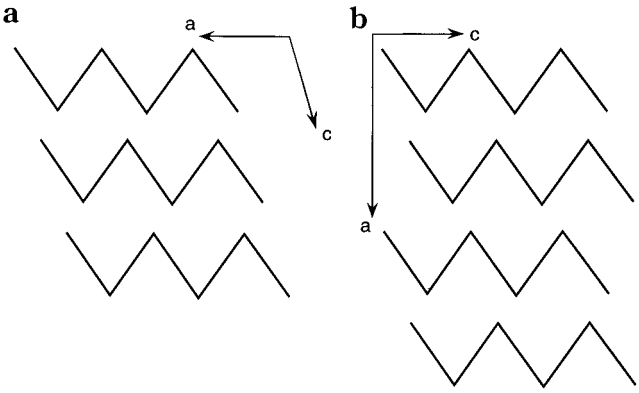

Figure 7. Stairs-like configuration of the HTB type layers parallel to (001) in $K_3V_{1.4}W_{2.6}O_9(PO_4)_2$ (a) and to (100) in $K_3Nb_3WO_9(PO_4)_2$ (b). The projections of the HTB ribbons along $\vec{b}$ are represented by segments that are 90° oriented alternately.

In both compounds, according to the formulas, the sum of the valencies for the transition metals is 21. No

Table 4

(a) Distances (Å) and Angles (deg) in the Polyhedra for $K_3V_{1.4}W_{2.6}O_9(PO_4)_2$[a]

W(1)	**O(1)**	**O(3)**	**O(4)**	**O(2^{i})**	**O(1^{ii})**	**O(4^{ii})**
O(1)	**1.81 (2)**	2.74 (3)	2.77 (3)	2.74 (3)	2.68 (2)	3.88 (3)
O(3)	95.7 (9)	**1.89 (3)**	2.67 (3)	3.73 (4)	2.74 (3)	2.67 (3)
O(4)	90.8 (8)	84.6 (9)	**2.08 (2)**	2.60 (2)	3.88 (3)	2.75 (3)
O(2^{i})	96.2 (8)	162 (1)	82.2 (8)	**1.88 (3)**	2.74 (3)	2.60 (2)
O(1^{ii})	95.6 (8)	95.7 (9)	173.6 (8)	96.2 (8)	**1.81 (2)**	2.77 (3)
O(4^{ii})	173.6 (8)	84.6 (9)	82.9 (7)	82.2 (8)	90.8 (8)	**2.08 (2)**

M(2) = 0.41(1)V + 0.59(1)W

M(2)	**O(2)**	**O(3)**	**O(5)**	**O(6^{iv})**	**O(6^{v})**	**O(5^{ii})**
O(2)	**1.88 (3)**	3.75 (4)	2.73 (3)	2.69 (3)	2.69 (3)	2.73 (3)
O(3)	174 (1)	**1.88 (3)**	2.79 (3)	2.69 (3)	2.69 (3)	2.79 (3)
O(5)	86.6 (8)	89.1 (8)	**2.09 (2)**	3.95 (2)	2.79 (2)	2.72 (2)
O(6^{iv})	91.9 (8)	91.7 (8)	170.5 (7)	**1.87 (2)**	2.87 (2)	2.79 (2)
O(6^{v})	91.9 (8)	91.7 (8)	89.5 (7)	99.9 (7)	**1.87 (2)**	3.95 (2)
O(5^{ii})	86.6 (8)	89.1 (8)	81.1 (7)	89.5 (7)	170.5 (7)	**2.09 (2)**

M(3) = 0.501(8)V + 0.499(8)W

M(3)	**O(7)**	**O(8)**	**O(6)**	**O(9)**	**O(10)**	**O(1^{iii})**
O(7)	**1.69 (2)**	2.70 (2)	2.69 (2)	2.86 (2)	2.75 (3)	3.82 (3)
O(8)	99 (1)	**1.87 (6)**	2.66 (2)	2.80 (2)	3.86 (2)	2.79 (3)
O(6)	97.8 (8)	90.4 (8)	**1.88 (1)**	3.88 (2)	2.70 (3)	2.62 (3)
O(9)	99.7 (8)	91.3 (8)	162.0 (9)	**2.05 (1)**	2.80 (2)	2.71 (2)
O(10)	95.0 (9)	166 (1)	87.3 (7)	86.8 (7)	**2.03 (2)**	2.62 (3)
O(1^{iii})	173.2 (8)	88 (1)	81.3 (8)	80.8 (7)	78.2 (8)	**2.13 (2)**

P(1)	**O(4^{vi})**	**O(9^{vii})**	**O(10^{viii})**	**O(5^{ii})**
O(4^{vi})	**1.53 (2)**	2.48 (3)	2.52 (3)	2.54 (3)
O(9^{vii})	109 (1)	**1.52 (2)**	2.57 (2)	2.43 (2)
O(10^{viii})	108 (1)	112 (1)	**1.58 (2)**	2.55 (3)
O(5^{ii})	112 (1)	106 (1)	110 (1)	**1.53 (2)**

K−O Distances (Å)

K(1)−O(5^{x}) = 2.74 (2)	K(2)−O(7^{ix}) = 2.77 (2)	K(1)−O(8) = 3.09 (3)	K(2)−O(6^{iv}) = 3.22 (2)
K(1)−O(5^{xi}) = 2.74 (2)	K(2)−O(4) = 2.89 (2)	K(1)−O(9^{xiii}) = 3.22 (2)	K(2)−O(1) = 3.30 (2)
K(1)−O(7^{viii}) = 2.99 (2)	K(2)−O(10^{iv}) = 2.90 (2)	K(1)−O(9^{i}) = 3.22 (2)	K(2)−O(3) = 3.34 (1)
K(1)−O(7) = 2.99 (2)	K(2)−O(5^{ii}) = 3.14 (2)	K(1)−O(3^{x}) = 3.23 (3)	K(2)−O(1^{xii}) = 3.35 (2)
K(1)−O(2^{iii}) = 3.07 (3)	K(2)−O(7^{viii}) = 3.18 (2)		K(2)−O(6^{viii}) = 3.35 (2)

Symmetry Code

i: 1 + *x*; *y*; *z*	v: 1 − *x*; 1 − *y*; 1 − *z*	viii: *x*; $^{1}/_{2}$ − *y*; *z*	xi: 1 − *x*; 1 − *y*; − *z*
ii: *x*; $^{3}/_{2}$ − *y*; *z*	vi: −1 + *x*; *y*; *z*	ix: 1 − *x*; $^{1}/_{2}$ + *y*; − *z*	xii: 2 − *x*; 1 − *y*; 1 − *z*
iii: 1 − *x*; $^{-1}/_{2}$ + *y*; 1 − *z*	vii: − *x*; $^{1}/_{2}$ + *y*; − *z*	x: 1 − *x*; $^{-1}/_{2}$ + *y*; − *z*	xiii: 1 + *x*; $^{1}/_{2}$ − *y*; *z*
iv: 1 − *x*; $^{1}/_{2}$ + *y*; 1 − *z*			

(b) Distances (Å) and Angles (deg) in the Polyhedra for $K_3Nb_3WO_9(PO_4)_2$[a]

M(1) = 0.89(2)Nb + 0.11(2)W

M(1)	**O(1^{i})**	**O(1^{iv})**	**O(2)**	**O(2^{iii})**	**O(3^{i})**	**O(4)**
O(1^{i})	**2.03 (2)**	2.79 (2)	3.90 (3)	2.74 (3)	2.68 (3)	2.83 (2)
O(1^{iv})	86.8 (7)	**2.08 (2)**	2.74 (3)	3.90 (3)	2.68 (3)	2.84 (3)
O(2)	172.7 (8)	89.1 (8)	**1.87 (2)**	2.75 (3)	2.69 (3)	2.76 (3)
O(2^{iii})	89.1 (8)	172.7 (8)	94.3 (9)	**1.87 (2)**	2.69 (3)	2.76 (3)
O(3^{i})	84.4 (7)	84.4 (7)	89.2 (8)	89.2 (8)	**1.96 (3)**	3.86 (3)
O(4)	92.3 (8)	92.3 (8)	93.8 (9)	93.8 (9)	175 (1)	**1.90 (3)**

M(2) = 0.46(2)Nb + 0.54(2)W

M(2)	**O(5^{i})**	**O(5^{ii})**	**O(6)**	**O(6^{iii})**	**O(3)**	**O(4^{i})**
O(5^{i})	**1.78 (2)**	2.79 (2)	3.91 (3)	2.75 (3)	2.74 (3)	2.76 (3)
O(5^{ii})	103.0 (8)	**1.78 (2)**	2.75 (3)	3.91 (3)	2.74 (3)	2.74 (3)
O(6)	167.7 (8)	88.3(8)	**2.14 (2)**	2.75 (3)	2.69 (3)	2.67 (3)
O(6^{iii})	88.3 (8)	167.0 (8)	80.0 (8)	**2.14 (2)**	2.69 (3)	2.67(3)
O(3)	98.1 (8)	98.1 (8)	84.6 (8)	84.6 (8)	**1.84 (2)**	3.77(3)
O(4^{i})	93.9 (8)	93.9 (8)	80.5 (8)	80.5 (8)	161 (1)	**1.98 (3)**

M(3) = 0.84(2)Nb + 0.16(2)W

M(3)	**O(5)**	**O(7)**	**O(8)**	**O(2)**	**O(9)**	**O(10)**
O(5)	**2.26(2)**	2.85 (2)	2.78 (3)	2.70 (3)	2.93 (3)	3.99 (3)
O(7)	82.4 (7)	**2.06(2)**	2.79 (2)	3.94 (3)	2.88 (3)	2.96 (3)
O(8)	80.8 (7)	86.1 (7)	**2.03(2)**	2.82 (3)	3.92 (3)	2.72 (3)
O(2)	79.9 (8)	162.4 (8)	90.9 (8)	**1.92(2)**	2.63 (3)	2.72 (3)
O(9)	89 (1)	93 (1)	169 (1)	87 (1)	**1.905(8)**	2.75 (3)
O(10)	171.6 (8)	102.0 (8)	92.3(8)	95.5 (9)	97 (1)	**1.74(2)**

P(1)	**O(1)**	**O(7^{v})**	**O(8)**	**O(6)**
O(1)	**1.55(2)**	2.48 (2)	2.49 (3)	2.57 (3)
O(7^{v})	107 (1)	**1.54(2)**	2.45(3)	2.56 (3)
O(8)	108 (1)	106 (1)	**1.52(2)**	2.53 (3)
O(6)	112 (1)	112 (1)	110.8 (8)	**1.55(2)**

K−O Distances (Å)

K(1)−O(6^{vi}) = 2.85 (2)	K(1)−O(9^{ix}) = 3.11 (4)	K(2)−O(10^{vii}) = 2.84(2)	K(2)−O(10^{ix}) = 3.20(2)
O(6^{vii}) = 2.85 (2)	O(3) = 3.23 (3)	O(1^{i}) = 2.99(2)	O(5^{i}) = 3.23(2)
O(10^{ix}) = 2.94 (2)	O(7^{i}) = 3.35 (2)	O(8) = 3.06(2)	O(2) = 3.26(2)
O(10^{x}) = 2.94(2)	O(7^{ii}) = 3.35 (2)	O(6^{ix}) = 3.20(2)	
O(4^{viii}) = 3.00 (3)			

Symmetry Codes

i: $^{1}/_{2}$ − *x*; 1 − *y*; $^{1}/_{2}$ + *z*	O(2) = 3.26(2)	vii: $^{1}/_{2}$ + *x*; *y*; $^{1}/_{2}$ − *z*	ix: $^{1}/_{2}$ − *x*; 1 − *y*; $^{-1}/_{2}$ + *z*
ii: $^{1}/_{2}$ − *x*; $^{1}/_{2}$ + *y*; $^{1}/_{2}$ + *z*	v: −*x*; 1 − *y*; −*z*	viii: 1 − *x*; 1 − *y*; 1 − *z*	x: $^{1}/_{2}$ − *x*; $^{1}/_{2}$ + *y*; $^{-1}/_{2}$ + *z*
iii: *x*; $^{1}/_{2}$ − *y*; *z*	vi: $^{1}/_{2}$ + *x*; $^{1}/_{2}$ − *y*; $^{1}/_{2}$ − *z*		

[a] The M−O or P−O bond lengths are on the diagonal, above it are the O···O distances and below it are the O−M−O or the O−P−O angles.

problem occurs concerning the repartition of the valence in the niobium compound, whose formula must necessarily be written $K_3Nb^{V}{}_3W^{VI}O_9(PO_4)_2$, i.e., with its transition elements entirely oxidized. It is more hazardous to propose a charge balance for $K_3V_{1.4}W_{2.6}O_9(PO_4)_2$ in which reduced species are necessarily present. As tungsten and vanadium are spread over the same sites in the structure, the valence calculations cannot be used. However, since the synthesis of the oxidized compound $K_3V_3WO_9(PO_4)_2$ has failed, one can suppose that the presence of V(IV) is necessary to stabilize the framework.

In both structures, the M(3) octahedra, which present one free corner, are less regular than the M(1) and M(2) octahedra. The M(3)−O distances are indeed ranging from 1.69 to 2.13 Å for $K_3V_{1.4}W_{2.6}O_9(PO_4)_2$ (Table 4a) and from 1.74 to 2.26 Å for $KNb_3WO_9(PO_4)_2$ (Table 4b), whereas the M(1)−O and M(2)−O distances are respectively ranging from 1.81 to 2.08 Å and from 1.87 to 2.09 Å in the vanadium compound (Table 4a) and from 1.79 to 2.14 Å and 1.858 to 2.03 Å for the niobium compound (Table 4b). Note that the mean values of these M−O bond lengths are shorter in the vanadium compound (1.928−1.947−1.941 Å) than in the niobium one (1.947−1.986−1.953 Å), in agreement with the values of the cell volumes corresponding to one formula unit (i.e., 367.1 and 381.9 $Å^3$, respectively).

The PO_4 tetrahedra present the classical geometry of monophosphate groups with P−O distances ranging from 1.52 to 1.58 Å in $K_3V_{1.4}W_{2.6}O_9(PO_4)_2$ (Table 4a) and from 1.52 to 1.55 Å in $K_3Nb_3WO_9(PO_4)_2$ (Table 4b).

The Intercalated Cations

The K(1) cations sit at the intersections of the large tunnels running along $\vec{b}$ and [101]. In both compounds K(1) has a 9-fold coordination with K(1)−O distances ranging from 2.74 to 3.23 Å in $K_3V_{1.4}W_{2.6}O_9(PO_4)_2$ (Table 4a) and from 2.85 to 3.35 Å in $K_3Nb_3WO_9(PO_4)_2$ (Table 4b). The K(2) ions are located in large cages with K(2)−O distances ranging from 2.77 to 3.35 Å and from 2.84 to 3.26 Å in the vanadium and niobium compounds, respectively. Thus, the mean K−O values are the same in both structures (3.09 Å), but one can observe shorter minimum K−O distances (2.744−2.774 Å) in the vanadium compound than in the niobium one (2.837−2.853 Å; Table 4a,b).

The size of the cages and of the tunnels in these frameworks allows us to insert larger cations than potassium. The Table 1 gives the cell parameters deduced from the X-ray powder diffraction patterns of $A_3V_2W_2O_9(PO_4)_2$ (with A = K, Rb, Tl, and Cs) and of $A_3Nb_3WO_9(PO_4)_2$ (with A = K, Rb, Cs). As expected, the cell volumes increase with the size of the insered cation.

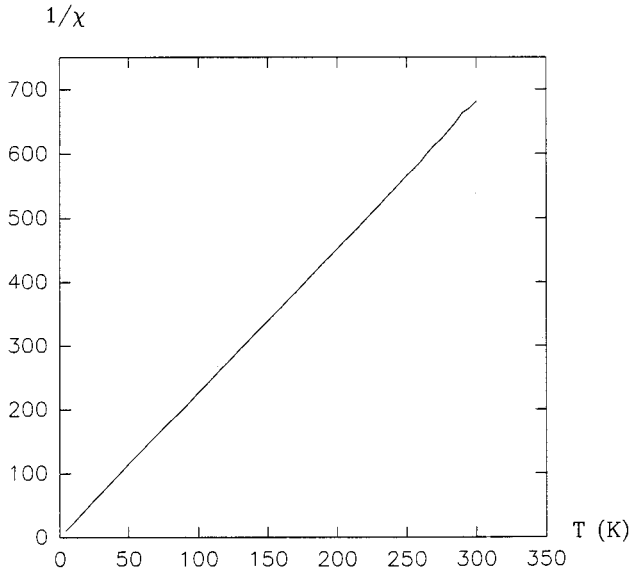

Figure 8. χ_m^{-1} versus T (K) for $K_3V_2W_2O_9(PO_4)_2$.

Magnetic Study of $K_3V_2W_2O_9(PO_4)_2$

The magnetic susceptibility of a powdered sample of $K_3V_2W_2O_9(PO_4)_2$ has been investigated by SQUID magnetometry in the 4.5−300 K temperature range. The zero field cooled magnetic moment of the sample was measured in a field of 0.3 T. The magnetic moment of the sample holder was measured in the same temperature range under the same magnetic field and was subtracted from the total measured moment.

The molar susceptibility have been fitted with the law $\chi = \chi_0 + C/(T - \theta)$, leading to a C parameter corresponding to 1.88 μ_B per d^1 ion, i.e., compatible with the expected value. This result indicates that there is an electronic localization on the vanadium and tungsten species despite the existence of $[MO_3]_\infty$ octahedral chains. This behavior is corroborated by the resistivity measurements which evidence that this phase is an insulator. Finally it must be noted, that the curve χ_m^{-1} versus T (Figure 8) does not show any magnetic ordering down to 4.5 K.

In conclusion, two new monophosphates with original intersecting tunnel structures have been isolated. The close structural relationships between these frameworks, which recall the chemical twinning phenomena, suggest that it should be possible to generate new members from the intergrowth of these structures. This study supports strongly the viewpoint according to which the association of two transition elements in the same phosphate matrix represents a very promising route for the generation of new frameworks.

CM970547L